Physica Scripta. Vol. T49, 605–609, 1993

Affecting Weak Light Localization by Strong Magnetic Fields

R. Lenke and G. Maret

Grenoble High Magnetic Field Laboratory, Max-Planck-Institut für Festkörperforschung and Centre National de la Recherche Scientifique, B.P. 166, F-38042 Grenoble-Cedex, France

Received March 30, 1993; accepted March 31, 1993

Abstract

We report an experimental study of the magneto-optical Faraday effect in strongly multiple scattering media using magnetic fields up to 23 Tesla. Faraday rotation of the polarization of laser light, diffusing through samples consisting of colloidal particles embedded in a Faraday-active glass matrix, is found to destroy coherent backscattering. The angular shape of the coherent backscattering cone varies as a function of the applied field B in agreement with a simple model and with numerical simulations. In particular, the intensity at backscattering is found to decrease with B like the intensity with scattering angle at $B = 0$, as predicted. The multiple scattering Faraday effect provides a unique experimental way to destroy constructive interferences between time reversed optical scattering paths. It is thus expected to affect light localization and may be used to prove (or disprove) its existence.

1. Introduction

Multiple scattering of both classical and quantum-mechanical waves results in enhanced backscattering, e.g. in a principally twofold increase of the backscattered intensity as compared to the diffuse intensity background at angles well off backscattering. This effect, also called coherent backscattering (CB), originates from the constructive interference between a wave travelling along any sequence of scattering events and its time-reversed sequence. CB is at the origin of "weak" or "strong" localization in electron transport in impure metals [1] and has been increasingly studied recently with classical waves such as light [2–5]. The angular width of the backscattering cone, which was found of order of the ratio of the wavelength λ to the transport mean free path l, is the key parameter describing the strength of this effect. In typical samples such as concentrated suspensions of submicron sized colloidal particles, paper and the like, λ/l is of order 10^{-2} or less. A transition to strong localization, where diffusion of waves over macroscopic distances ($\gg l$) becomes essentially suppressed by CB, is expected [6] to occur around $\lambda/l \approx 2\pi$. Attempts to reach this transition for visible light were unsuccessful so far, basically because of (i) the very restricted range of particle size, wavelength, volume fraction and refractive index, where optical localization may be expected, (ii) substantial renormalization of l due to interparticle position correlations (see e.g. [7]) and (iii) the large reduction in the speed of wave propagation due to resonant Mie-scattering [8], which explains the anomalously small diffusion constant observed [9].

It has been suggested [10, 11], that the magneto-optical Faraday effect (FE) will suppress CB, because it breaks the reversibility of light propagation and may thus act as an optical diode [12]. This effect, which would allow to evaluate the contribution of CB to the wave transport and hence to probe the vicinity of the transition to strong localization, has been observed recently in very strong magnetic fields [13]. Using fine powders of rare earth doped paramagnetic Faraday rotator glasses, the backscattering cone was decreased by about 40% and the transmission speckle patterns almost completely changed at $B = 23$ Tesla. These experiments were carried out at temperatures between 30 K and 70 K in order to obtain sufficient Faraday rotation. The required volume fractions of particles ranged between about 20% and 40%, where interparticle correlations play a significant role. In addition, FE was caused by the scattering particles themselves, and they had both irregular shapes and a rather broad size distribution. All this makes a quantitative analysis of this data set very difficult. The opposite case of non-Faraday-active scatterers embedded in a Faraday-active background appears conceptually much easier and, in fact, all theoretical models existing so far [10, 11, 13] rather apply to this situation.

We report here a new series of experiments on destruction of CB, using monodisperse spherical silica particles surrounded by an essentially homogeneous matrix of Faraday rotator glass. The volume fractions of SiO_2-particles and matrix material were about $\Phi_s = 1\%$ and $\Phi_F = 90\%$, respectively, providing larger l-values and larger FE than in the previous work. Since the magnitude of the effect increases with $V\Phi_F lB$, as outlined below, V being the Verdet constant of the bulk material, these experiments could be performed at room temperature, which substantially improves the data quality for a number of technical reasons. We find that the magnetic field induced change of the angular shape of the backscattering cone at small angles is in good agreement with our recent model [13] and with simple numerical simulations described below. In particular, we verify experimentally one of the most important predictions of the photon diffusion model: that the enhancement factor of the backscattered intensity (at $q = 0$) should decay, as a function of VBl, like the scattered intensity at $B = 0$ as a function of the scattering angle Θ off backscattering, when scaled as ql, $q = 4\pi \sin(\Theta/2)/\lambda$ being the scattering vector.

2. Multiple scattering Faraday effect

2.1. *Physical concept*

The linear polarization of light propagating along a distance s in a homogeneous Faraday-active medium is rotated by

an angle $\alpha = \boldsymbol{VB} \cdot \boldsymbol{s}$. Accordingly, circularly polarized light is phase-shifted by α. Reversing the direction of light propagation ($\boldsymbol{s} \rightarrow -\boldsymbol{s}$) reverses the sense of rotation with respect to the direction of light propagation ($\alpha \rightarrow -\alpha$). Thus, for example, in a Fabry–Perot type device, where light is reflected, say, N times between two parallel mirrors at distance d, α is simply proportional to the total path length Nd. In multiple scattering, the situation is less straightforward because of the different successive polarization changes which occur on scattering along a tortuous scattering path. The relationship between the input and output polarization states of individual scattering events is completely deterministic and well known, both for Rayleigh- and Mie-scatterers; it strongly depends on the relative orientations of the incoming and outgoing scattering vectors, resulting in a wide distribution of polarization states for an ensemble of random multiple scattering paths. In fact, the incident polarization state is lost on a distance of the order of l. It is important to notice that – unlike in a Fabry–Perot – a rotation by $\delta\alpha$ (for example due to FE) of the input polarization state at a given scattering event does not result, in general, in a simple rotation by $\delta\alpha$ of the output polarization state. For example, in Rayleigh scattering, $\delta\alpha$ becomes $\delta\alpha$ at forwardscattering, but $-\delta\alpha$ at backscattering. Therefore, if we consider a random distribution of input polarization states and scattering vectors – as occurring in high order multiple scattering – we may expect a distribution of rotations of output polarizations with zero mean and variance $\approx \delta\alpha^2$. The exact distribution function obviously depends on the specific properties of the scatterers. As, in multiple scattering, the characteristic distance for straight propagation is l, the typical mean square Faraday rotation per scattering along a random path should be of order $(VBl)^2/3$. Thus, in this very simple minded picture, Faraday rotation in multiple scattering does not add up, on average, according to $\sum_i \boldsymbol{s}_i \boldsymbol{B}$ along an ensemble of random scattering paths of length s, but averages to zero with variance $s/l \cdot (VBl)^2/3$.

2.2. *A simple model*

So far, there is no theory of the multiple scattering FE, which properly accounts for the scattering vector dependent polarization transfer on individual scattering events, neither for Rayleigh- nor for Mie-particles. To describe how FE acts on CB, Golubentsev [10] studied a randomly inhomogeneous gyrotropic medium, MacKintosh and John [11] considered magnetic field induced phase shifts on (left or right) circularly polarized states and random helicity flips between them at each scattering. A multiple Mie-scattering Monte Carlo simulation study has been performed recently [15]. The physical picture discussed above suggests the following simple model [13] which contains, we think, the essential ingredients to describe qualitatively the multiple scattering FE. According to Akkermans *et al.* [16], the angular dependence of the coherent enhancement of the scattered light intensity $I(q)$ can be written as a continuous sum over all scattering paths like

$$I(q) = 1 + \frac{1}{I(0)} \int_l^\infty P(s) e^{-(s/3l) \cdot q^2 l^2} \, ds \tag{1}$$

s is the path length and $P(s)$ a geometry dependent weighting function, which for reflection from a very thick slab decays as $P(s) \approx s^{-3/2}$ in the diffusion approximation. This gives

$$I(q) = 1 + \frac{(1 - e^{-2\gamma q l})}{2\gamma q l} \tag{2}$$

γ is a coefficient of order unity (5/3 in Ref. [16]). There are various other expressions for $I(q)$ in the literature; we use eq. (2) here, because it is simple, agrees rather well with experiments [14] and makes evident the average contribution of paths of lengths s which allows to incorporate easily the FE. The difference in Faraday rotation angle between reversed paths, per step l, is of order $\delta\alpha = 2VBl \cos\theta$, θ being the angle between $\boldsymbol{B}$ and the local direction of propagation. This gives a θ-averaged contribution of $\langle 1 + \cos(\delta\alpha)\rangle_\theta \approx 1 + \exp(-2V^2B^2l^2/3)$ to $I(q)$. Under the assumption of no correlations between the $\delta\alpha$'s of consecutive steps, the average contribution of paths of length s becomes $1 + \exp(-s/l \cdot 2V^2B^2l^2/3)$. Since the phase shifts between reversed paths due to FE are independent of phase shifts due to variations of the external scattering angle Θ, we can write for $I(q, B)$ in the presence of FE

$$I(q, B) = 1 + \frac{1}{I(0, 0)} \int_l^\infty P(s) e^{-(s/3l) \cdot (q^2l^2 + 2V^2B^2l^2)} \, ds \tag{3}$$

and hence

$$I(q) = 1 + \frac{(1 - e^{-2\gamma\sqrt{x}})}{2\gamma\sqrt{x}} \tag{4}$$

with $x = q^2l^2 + 2V^2l^2B^2$. Absorption can be easily incorporated by an exponential damping with absorption length l_a along the path [13, 14]. Equation (4) is plotted as a function of $\sqrt{x}$ in Fig. 2. These expressions illustrate the equivalence of the scaled scattering angle ql and the scaled Faraday rotation angle $\sqrt{2}\,VlB$ and predict that (i) the triangular shape of the CB-cone should be rounded off by the FE and (ii) the enhancement at backscattering $I(0, B)$ should decay with increasing $\sqrt{2}\,VBl$ like the CB-cone $I(q, 0)$ with ql. We expect that these two features would qualitatively hold also for more sophisticated models. However, the numerical coefficient ($\sqrt{2}$ here) relating ql and VBl could come out different and a correlation length of FE could appear explicitly (in the above model this length was put equal to l).

2.3. *A simple numerical simulation*

We have compared the above model with a very simple numerical simulation. We consider isotropic scattering (from points) as generated by a random choice of two polar angles at each scattering event. The distance r between successive scattering events is randomly chosen according to the weight distribution $\exp(-r/l)$. The sample is a semi-infinite slab of thickness $L = 100 \cdot l$, the first scattering occurs at $\boldsymbol{r}_i$ with $x = 0$, $y = 0$ and at a depth z from the entrance surface ($z = 0$) randomly selected with weight $\exp(-z/l)$. A scattering path is terminated (at $\boldsymbol{r}_a$) whenever the next scattering event happened to occur outside the slab ($z < 0$, $z > L$). $I(q)$ is evaluated by averaging $1 + \cos[\boldsymbol{q} \cdot (\boldsymbol{r}_a - \boldsymbol{r}_i)]$ over 10000 paths. We verified that $p(s)$ decays like $s^{-3/2}$ (no absorption) and obtain reasonable values for the transmission coefficient (0.0178, $\approx \gamma l/L$) and for the single scattering contribution to the reflection coefficient (0.16). We do not keep track of the local polarization state. Rather, we

just consider circularly polarized light of identical helicity for the pair of reversed waves and monitor their phases. Faraday rotation is included as a phase shift $\delta\alpha = \pm VBr\cos(\theta)$ per step on each of the two waves. The scattering vector dependent relationship between the FE-induced changes of input and output polarization states at each scattering event is buried into a random choice of the sign of $\delta\alpha$, as suggested by MacKintosh and John [11]. A continuous distribution function for $\delta\alpha$ with characteristic width of order VBl would presumably be closer to physical reality, but is not expected to lead to qualitatively different properties of the multiply scattered light. Figure 1 shows $I(q, B)$ as a function of the scaled scattering angle ql. The contribution of single scattering was subtracted off, since it just adds a flat background. We clearly observe – with increasing B – a lowering of the coherent backscattering enhancement as well as a rounding of the triangular tip of the cone at small q. In Fig. 2 we compare $I(q)$ *vs.* ql at $B = 0$ with $I(0, B)$ *vs.* $\sqrt{2}\,VBl$ at backscattering. Both functions decay in a very similar way. These features qualitatively corroborate the simple model outlined above. For comparison we have also plotted in Fig. 2, $I(ql, 0) \equiv I(0, \sqrt{2}\,VBl)$ according to eq. (4). The prediction of this model agrees surprisingly well with the simulations. The small differences between the two simulations and eq. (4), which seem to become more significant at larger arguments, may be due to the particular description of the scattering near the sample surface.

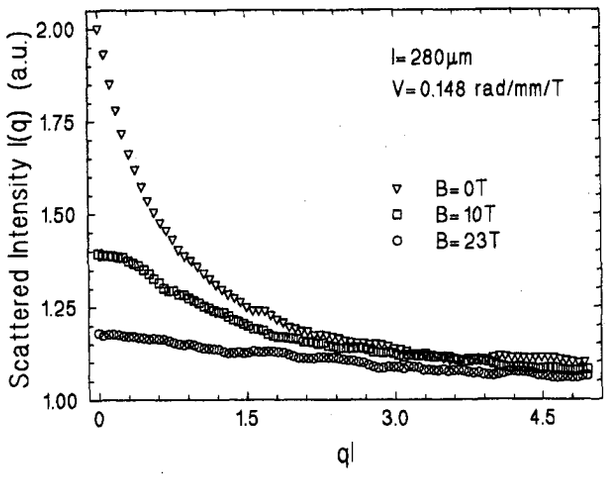

Fig. 1. Numerical simulation of the magnetic field dependent angular shape of the coherent backscattering cone. The parameters l and V correspond to the experimental values for the data set shown in Fig. 3.

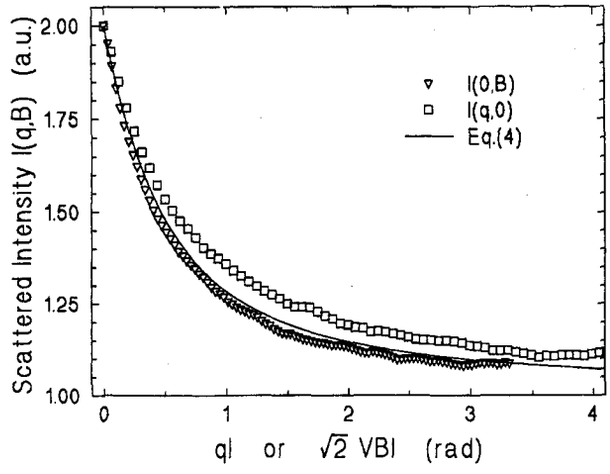

Fig. 2. Comparison of simulation and eq. (4). (□) Angular dependence of the cone, $I(q, 0)$ *vs.* ql, at $B = 0$, simulation. (▽) Magnetic field dependence of the enhancement factor, $I(0, B)$ *vs.* $\sqrt{2}\,VBl$, at backscattering, simulation. Continuous line: $I(q, 0)$ *vs.* ql and, equivalently, $I(0, B)$ *vs.* $\sqrt{2}\,VBl$ according to eq. (4).

3. Experimental

Free standing disk-shaped solid samples of 13 mm diameter and 5 mm thickness were prepared by mixing 0.09 μm diameter silica beads with a fine powder of Faraday rotator glass FR5 from Hoya (Japan) [13] and melting of the FR5-glass by heating for 5 min to 900 °C. The volume fractions were $\Phi_s = 1\%$ and $\Phi_F = 90\%$, the remainder being due to incorporated air bubbles. Circular or linear polarized light of an Ar^+-laser ($\lambda = 0.457\,\mu m$) was expanded to a 10 mm diameter beam impinging on the sample after 90°-reflection from a 50% transmission beamsplitter. Samples were placed in the central part of a resistive polyhelix solenoid providing steady magnetic fields up to 23 Tesla. The light scattered around the backscattering direction was passed through a linear or circular analyser and focused by a 500 mm focal distance lens on a 8 bit 512 by 512 pixel CCD video camera positioned in the focal plane. Speckle patterns were averaged out by rotation of the sample about the normal to its surface and adding 255 video frames. In order to correct for small distortions of the beams scattered to wider angles, the resulting pictures were normalized to pictures from samples with CB-cones too narrow to resolve. Intensities were azimuthally averaged around the pixel of maximum intensity (tip of the cone) and normalized to the flat wide angle background. As this background also contains parasitic stray-light and single backscattering, experimental enhancement factors at $B = 0$ were smaller than 2 (between 1.4 and 1.8). In order to compare different data sets, we have renormalized the enhancement to the same $I(0, 0)$.

4. Experimental results

Figure 3 shows a series of coherent backscattering cones as obtained at different magnetic fields. The cone shape at $B = 0$ is not completely triangular at backscattering because of residual absorption [14]. The cone height decreases with increasing B and the top becomes progressively rounded, as predicted by our model and in agreement with the simulations shown in Fig. 1. This directly illustrates that weak localization of light, which manifests itself in CB, can be destroyed by laboratory strength magnetic fields. Long scattering paths, which essentially contribute to the small angle part of the cones, are more severely affected than shorter paths. The incoherent wide angle intensity $I(ql \gg 1)$ was found independent of B indicating that the FE acts only on the relative phase between time reversed paths, again as expected. Note that this differs from the effect of absorption on CB, which – in addition to the rounding – lowers the wide angle intensity [14].

In Fig. 4 we have plotted the height of the cone ($q = 0$) as a function of VB for the same sample at $T = 300\,K$ and at $T = 30\,K$. The corresponding Faraday rotation $V(B) \cdot B$, as measured independently on bulk FR5-samples, is linear in B

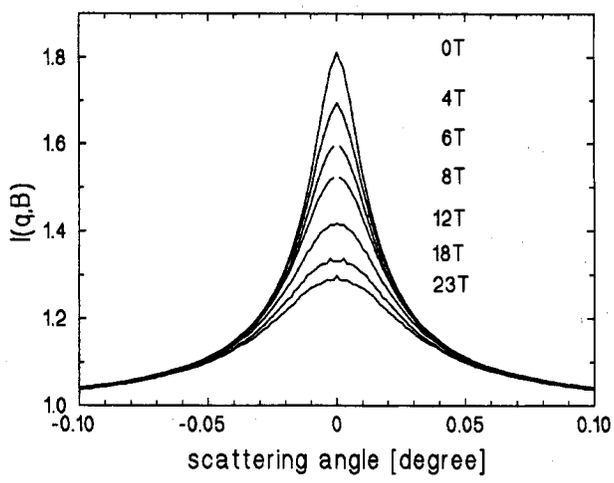

Fig. 3. Measured angular dependence of the scattered light intensity in the vicinity of backscattering ($\Theta = 0$) in different magnetic fields. Room temperature, $\lambda = 457.9$ nm, identical circular polarization of incident and detected beams. Sample: 180 nm diameter silica beads at 1% volume fraction in FR5-glass, transport mean free path $l \approx 280\,\mu$m.

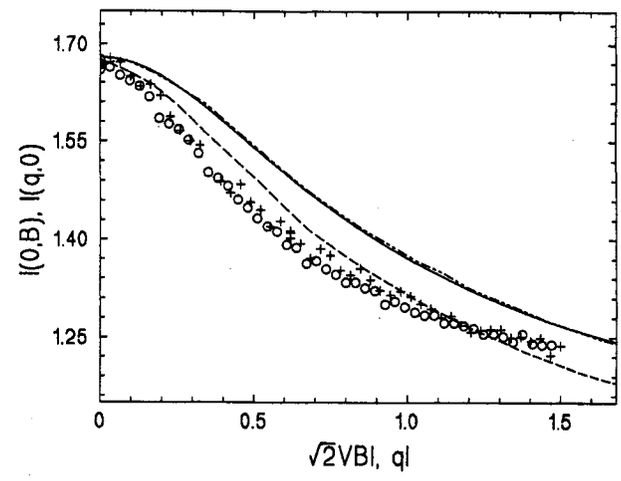

Fig. 5. Symbols: B-dependence on the backscattered intensity $I(0, B)$ *vs.* $\sqrt{2}\,VBl$, (○) identical circular and (+) identical linear polarization of incident and detected beams. Dashed lines: q-dependence of the scattered intensity at zero magnetic field, $I(q, 0)$ *vs.* ql, (– – –) circular and (–––·––) linear polarization, all for the sample described in Fig. 3, $T = 300$ K. Continuous line: Fit of (–––·––) to eq. (4).

at 300 K (slope 0.165 rad mm^{-1}T^{-1}), but at $T = 30$ K it becomes much stronger (slope 4.52 rad mm^{-1}T^{-1} at small B) and saturates at high fields. Despite of this, both data sets, obtained by variation of B, superimpose. This illustrates that the cone height $I(0, B)$ indeed scales with VB as suggested by the above simple model. The weak rounding observed at small VB can be attributed to residual absorption [13].

We have also studied the effect for different incident and detected polarization states. Figure 5 shows a comparison of the decay of the CB cone height for circular incident/circular detected light of identical helicity with linear incident/parallel linear detected light. Both data sets superimpose very well, as expected in a photon diffusion model for situations where contributions from long paths predominate and contributions of single backscattering are small, since long paths are completely depolarized. In fact, we found that for linear incident polarization, the maximum height of the cone is observed at an orientation of the linear analyser which increases with increasing magnetic field. For this sample, the rotation was 1.12 mrad/T, which combined with the V-value corresponds to a distance of 270 μm. Since this is close to the transport mean free path ($l \approx 280\,\mu$m), we might suggest that the Faraday rotation near the sample surface, that is before the first and after the last scattering event – which have an average distance of order l from the surface – might be responsible for this effect. The field induced rotation implies a small correction (<2.5% at 23 T) of the cone height measured at parallel polarizer and analyser, which is included in Fig. 5.

Figure 5 also shows the angular dependence of the CB-cones without magnetic field for the two sets of polarizations. The decay of $I(q, 0)$, when plotted against the reduced scattering angle ql, is very similar to the decay of the backscattered intensity when plotted against the reduced Faraday angle $\sqrt{2}\,VBl$. This is again consistent with the prediction of the simple model and with the numerical simulations. It suggests in fact that the typical correlation length of the Faraday rotation in the multiple scattering regime is indeed very close to the transport mean free path l, as assumed in our model. This conclusion is obviously independent of the value of l, since l enters only as a common scaling factor on the abscissa of both curves.

Finally Fig. 5 shows a fit of eq. (4) with $x = q^2l^2 + 3l/l_a$ [14] to the angular dependence of $I(q)$ of the cone for linear polarization, using $\gamma = 5/3$. This gives $l_a = 3.05$ mm and $l = 280\,\mu$m. The latter value was used to scale the abscissa. It compares well with the value $l = 290\,\mu$m calculated from the Mie transport cross section [14] and the volume fraction $\Phi_s = 0.01$. It thus appears that our simple description of the multiple scattering FE provides a fair, almost quantitative account for our data.

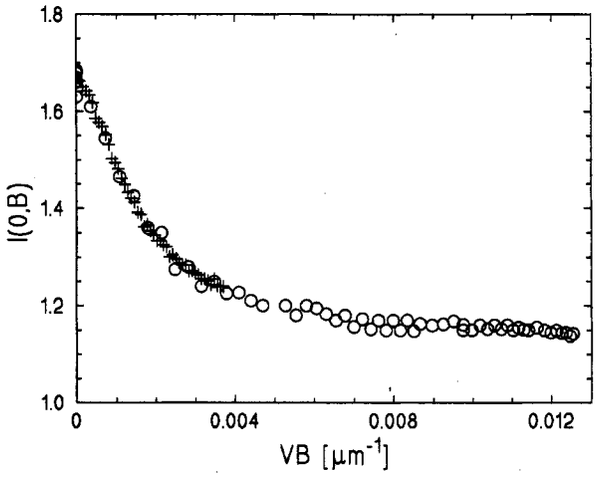

Fig. 4. Magnetic field dependence of the backscattered intensity $I(0, B)$ *vs.* VB for the sample described in Fig. 3. (+) $T = 300$ K; (○) $T = 30$ K.

5. Conclusions

The observation of substantial reduction of the coherent backscattering cone of visible light due to the Faraday effect provides first direct evidence that the CB phenomenon originates from interference of time reversed optical scattering paths. It shows that weak light localization can be strongly affected by laboratory strength magnetic fields. The effect

scales with the product of Verdet constant, transport mean free path and magnetic field strength, as suggested by a simple model and numerical simulations, and becomes therefore largest in samples with Faraday rotation in the background matrix, at small volume fractions of scatterers and high fields. It opens in principle the possibility to affect the expected transition to strong optical localization and thereby to prove (or disprove) its existence, although this will require very different experimental conditions (e.g. small l) which may be difficult to realize.

Acknowledgements

We thank R. Maynard and A. Martinez for many fruitful discussions. One of us (R.L.) acknowledges a doctoral grant from the University J. Fourier, Grenoble.

References

1. Bergmann, G., Phys. Rep. **107**, 1 (1984).
2. van Albada, M. P. and Lagendijk, A., Phys. Rev. Lett. **16**, 2692 (1985).
3. Wolf, P. E. and Maret, G., Phys. Rev. Lett. **55**, 2696 (1985).
4. Sheng, P. (Editor), "Scattering and Localization of Classical Waves in Random Media" (World Scientific Publishing, London 1990).
5. Soukoulis, C. M. (Editor), "Localization and Propagation of Classical Waves in Random and Periodic Structures" (Plenum, New York 1993).
6. Anderson, P. W., Phil. Mag. **52**, 505 (1985).
7. Fraden, S. and Maret, G., Phys. Rev. Lett. **65**, 512 (1990).
8. van Albada, M. P., van Tiggelen, B. A., Lagendijk, A. and Tip, A., Phys. Rev. Lett. **66**, 3132 (1991).
9. Drake, J. M. and Genack, A. Z., Phys. Rev. Lett. **63**, 259 (1991).
10. Golubentsev, A. A., Sov. Phys. JETP **59**, 26 (1984).
11. MacKintosh, F. P. and John, S., Phys. Rev. **B37**, 1884 (1988).
12. Lord Rayleigh, Phil. Trans. **176**, 343 (1885); Scientific Papers **2**, 360 (1900) and **3**, 163 (1902), Cambridge.
13. Erbacher, F. A., Lenke, R. and Maret, G., Europhys. Lett. **21**, 551 (1993).
14. Wolf, P. E., Maret, G., Akkermans, E. and Maynard, R., J. Phys. (Paris) **49**, 63 (1988).
15. Martinez, A. S. and Maynard, R., "Soft Order in Physical Systems" (Edited by R. Bruinsma and Y. Rabin) (Plenum, New York, to appear).
16. Akkermans, E., Wolf, P. E. and Maynard, R., Phys. Rev. Lett. **56**, 1471 (1986).